



Cite this: *Chem. Commun.*, 2014, 50, 13537

Received 25th July 2014,  
Accepted 29th August 2014

DOI: 10.1039/c4cc05719h

www.rsc.org/chemcomm

## Conductive porphyrin helix from ternary self-assembly systems†

Qiang Zhao,<sup>ab</sup> Yao Wang,<sup>ac</sup> Yan Qiao,<sup>ab</sup> Xiaolong Wang,<sup>ab</sup> Xuefeng Guo,<sup>ab</sup> Yun Yan<sup>\*ab</sup> and Jianbin Huang<sup>\*ab</sup>

**A helix with the ternary components of TPPS<sub>4</sub>, Zn(NO<sub>3</sub>)<sub>2</sub> and C<sub>14</sub>DMAO is easily obtained in aqueous solution. It retains the characteristic fluorescence of the porphyrin and can be conductive when it bridges on a gold electrode, which provides potential applications in photochemistry and electrical devices.**

Helix is ubiquitous in nature and have exclusive biological functions in living systems.<sup>1</sup> These helical structures represent ordered structures and consist of multiple components,<sup>2</sup> such as DNA, peptides and proteins, which are precisely arranged with multi-components.<sup>3</sup> To obtain these interesting helical structures, self-assembly is developed as one of the vital approaches.<sup>4</sup> Self-assembled helices<sup>5</sup> are particularly popular for their applications in biomaterials,<sup>6</sup> optoelectronics,<sup>7</sup> and catalysis.<sup>8</sup> Although there are some reports related to an artificial helix, most of them are concerned with mono-<sup>9</sup> or bi-component<sup>10</sup> systems, which are distinguished with natural multi-component helices. Therefore, it is still a great challenge to build ternary or multi-component helices by supramolecular chemistry.

Porphyrins have attracted considerable interest in functional molecular assemblies because of the diverse utilization in catalysis,<sup>11</sup> photomedicine<sup>12</sup> and material science.<sup>13</sup> Especially, some porphyrin structures have been constructed for photoconductors<sup>14</sup> and photovoltaics.<sup>15</sup> Schwab and co-workers researched on porphyrin nanorods, which could generate photoconductivity upon light exposure.<sup>16</sup> Wasielewski *et al.* synthesized modified zinc porphyrins that produced long-lived charge separation in the segregated  $\pi$ -stacks and charge migration through the columnar structure.<sup>17</sup> However, a little attention has been paid to the conducting properties of these self-assembled nanostructures.

Herein, we report a helical structure based on ternary molecular self-assembly of tetrasodium *meso*-tetra(sulfonatophenyl)porphine (TPPS<sub>4</sub>), zinc ions and tetradecyldimethylamine oxide (C<sub>14</sub>DMAO) in aqueous solution. As shown in the scanning electron microscopy (SEM) images (Fig. 1), both the left-handed and right-handed helix are single stranded (Fig. 1a and b), double stranded (Fig. 1c and d) and even multi-stranded (Fig. 1e and f) structures. The low magnification image indicates that they are hundreds of micrometers in length, 150–950 nm in diameter (average 440 nm, Fig. S1, ESI†). The transmission electron microscopy (TEM) image also confirms the helical structure formation in the TPPS<sub>4</sub>–Zn(NO<sub>3</sub>)<sub>2</sub>–C<sub>14</sub>DMAO system (Fig. S2, ESI†). TPPS<sub>4</sub>, Zn(NO<sub>3</sub>)<sub>2</sub> and C<sub>14</sub>DMAO are all indispensable to construct helix that the helical structure could not be obtained when any component is lacking.

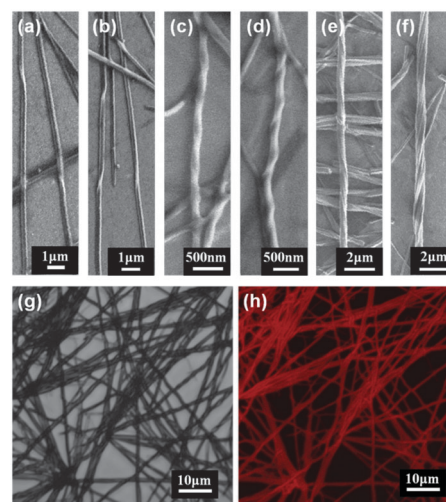


**Fig. 1** SEM images of TPPS<sub>4</sub>–Zn(NO<sub>3</sub>)<sub>2</sub>–C<sub>14</sub>DMAO deposited from the solution on a silicon slice: (a), (b) the single stranded helices, scale bar = 1  $\mu$ m; (c), (d) the double stranded helices, scale bar = 500 nm; and (e), (f) the multi-stranded helices, scale bar = 2  $\mu$ m. (g) The optical image and (h) fluorescent image of TPPS<sub>4</sub>–Zn(NO<sub>3</sub>)<sub>2</sub>–C<sub>14</sub>DMAO deposited onto a glass slide. Helices were achieved in the solution of TPPS<sub>4</sub> ( $1.0 \times 10^{-4}$  M), Zn(NO<sub>3</sub>)<sub>2</sub> ( $1.0 \times 10^{-4}$  M) and C<sub>14</sub>DMAO ( $2.0 \times 10^{-4}$  M).

<sup>a</sup> Beijing National Laboratory for Molecular Sciences (BNLMS), College of Chemistry and Molecular Engineering, Peking University, Beijing 100871, People's Republic of China. E-mail: JBHuang@pku.edu.cn

<sup>b</sup> State Key Laboratory for Structural Chemistry of Unstable and Stable Species, Peking University, Beijing 100871, People's Republic of China

<sup>c</sup> Key Laboratory of Polymer Chemistry and Physics of the Ministry of Education, Peking University, Beijing 100871, People's Republic of China

† Electronic supplementary information (ESI) available. See DOI: 10.1039/c4cc05719h

The helices retain the fluorescent properties of the porphyrin. Confocal laser scan microscopy (CLSM) offers the optical and fluorescent images of the helical structures in solution, which possessed red fluorescence (Fig. 1g and h and Fig. S3, ESI†). The fluorescent intensity of the solution, with addition of C<sub>14</sub>DMAO, increased first until the maximum was reached at about 4.0 equiv. C<sub>14</sub>DMAO, probably because of the enhancement of TPPS<sub>4</sub>-Zn(NO<sub>3</sub>)<sub>2</sub>-C<sub>14</sub>DMAO aggregation (Fig. S4, ESI†). After adding more than 4.0 equiv. C<sub>14</sub>DMAO, the fluorescence intensity decreased accompanied with the destruction of aggregates. The turbidity had a similar variation trend with the fluorescent intensity (Fig. S5, ESI†).

Current-voltage (*I-V*) measurements were performed to measure the conductivity of the helix. The device was designed with one helix bridging two Au electrodes (Fig. 2a and b). The resulting *I-V* curve exhibited a nearly linear correlation (Fig. 2c) in which a larger current was generated when a higher voltage was applied. The conductivity ( $\sigma$ ) of a single helix was calculated by the following formula:

$$\sigma = \frac{IL}{VS} \quad (1)$$

here, *V* is the voltage, *I* is the current, *S* is the average cross sectional area, which is estimated by assuming that the cross section of the helix is a cylinder, and *L* is the length of the helix between electrodes. For the device measured, the conductivity of the helix is about  $3.95 \times 10^{-5} \text{ S cm}^{-1}$ , which is comparatively higher than those of porphyrin structures.<sup>16,18</sup> The conductivity of the helix is attributed to the overlap of molecular HOMO and LUMO orbitals.<sup>9,19</sup> Therefore, the molecular arrangement of the helices is supposed that each porphyrin has interactions and forms helical alignments. These helices are anticipated to meet the special structural requirements for electronic and sensor device fabrication.

UV-vis spectroscopy and X-ray photoelectron spectroscopy (XPS) were employed to access the molecular arrangement within helices.

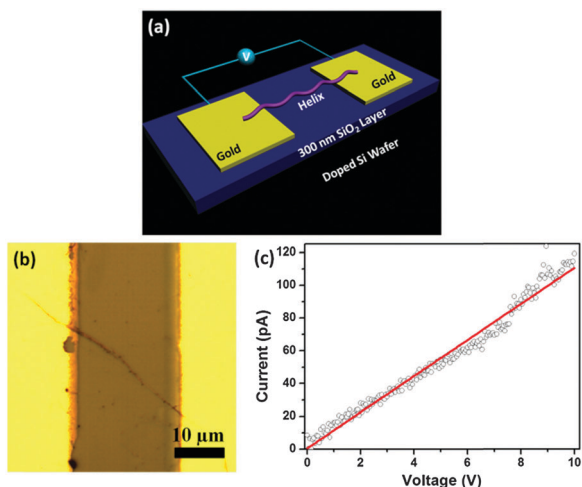


Fig. 2 (a) Scheme and (b) optical image of electrodes connected by a helix, where the silicon wafer acted as a global back-gate, scale bar = 10  $\mu\text{m}$ ; and (c) *I-V* curve of a helix deposited across a pair of Au electrodes separated by  $\sim 20 \mu\text{m}$  at a gate bias of 0 V.

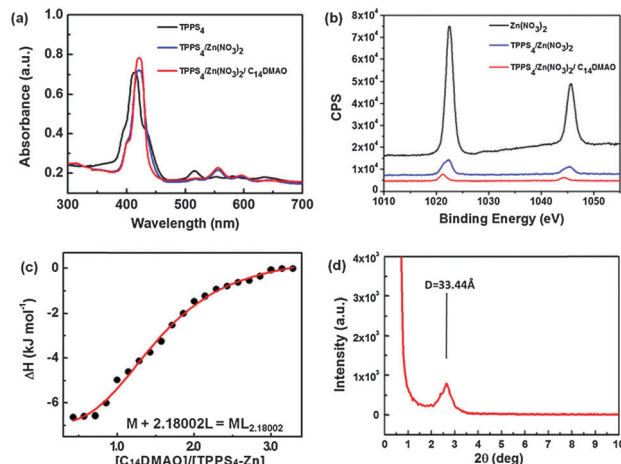


Fig. 3 (a) UV-vis spectra of TPPS<sub>4</sub>-Zn(NO<sub>3</sub>)<sub>2</sub>-C<sub>14</sub>DMAO system. TPPS<sub>4</sub> solution ( $5.0 \times 10^{-6} \text{ M}$ ) (black); TPPS<sub>4</sub> solution with the addition of Zn(NO<sub>3</sub>)<sub>2</sub> ( $5.0 \times 10^{-6} \text{ M}$ ) (blue), and the TPPS<sub>4</sub>/Zn(NO<sub>3</sub>)<sub>2</sub>/C<sub>14</sub>DMAO at the ratio of 1/1/2 ( $C_{14}\text{DMAO} = 1.0 \times 10^{-5} \text{ M}$ ) (red) at 25 °C. (b) The XPS measurement of Zn 2p peak for Zn(NO<sub>3</sub>)<sub>2</sub> (black), TPPS<sub>4</sub>-Zn(NO<sub>3</sub>)<sub>2</sub> (blue) and the helices of TPPS<sub>4</sub>-Zn(NO<sub>3</sub>)<sub>2</sub>-C<sub>14</sub>DMAO (red) deposited on the silicon substrate, respectively. (c) Fitted binding isotherms for the calorimetric titration of TPPS<sub>4</sub>-Zn(NO<sub>3</sub>)<sub>2</sub> ( $X_{\text{TPPS}_4} = 0.5$ ) with C<sub>14</sub>DMAO. (d) XRD patterns of the helices on glass sheet.

Concretely, the formation of zinc porphyrin was demonstrated by the UV-vis spectra (Fig. 3a). The Q band of TPPS<sub>4</sub> (557 nm and 596 nm) corresponding to the S<sub>0</sub> → S<sub>1</sub> transition is essentially ascribed to the formation of TPPS<sub>4</sub>-Zn(NO<sub>3</sub>)<sub>2</sub> in which the zinc ion occupies the central cavity of the porphyrin.<sup>20</sup> The enhancement of the Soret band is attributed to the Mie effect.<sup>21</sup> In the XPS spectra (Fig. 3b), 2p spectrum of zinc in TPPS<sub>4</sub>-Zn(NO<sub>3</sub>)<sub>2</sub> suggests that the spin-orbit pair with the 2p<sub>3/2</sub> component appearing at 1022.36 eV is due to the zinc oxidation state. In TPPS<sub>4</sub>-Zn(NO<sub>3</sub>)<sub>2</sub>-C<sub>14</sub>DMAO, a large chemical shift to a lower binding energy was observed in the Zn 2p spectrum at 1021.25 eV,<sup>22</sup> indicating the zinc ion was coordinated to the oxygen of C<sub>14</sub>DMAO, as well as the Zn-O coordination was based on an axial ligand to the metal porphyrin. In addition to, no obvious porphyrin-porphyrin stacking peak appeared in the UV-vis spectrum because the affinity of the zinc porphyrin to C<sub>14</sub>DMAO would lead to a weak  $\pi$ - $\pi$  interaction among each porphyrin.

For the construction of the ternary component helix, C<sub>14</sub>DMAO was added to the aqueous solution of TPPS<sub>4</sub> and Zn(NO<sub>3</sub>)<sub>2</sub> in a molar ratio of TPPS<sub>4</sub>/Zn(NO<sub>3</sub>)<sub>2</sub>/C<sub>14</sub>DMAO = 1/1/2. Isothermal titration calorimetry (ITC) measurements were performed to confirm this optimal ratio and the binding curve (Fig. 3c) and also provided the binding ability of C<sub>14</sub>DMAO with TPPS<sub>4</sub>-Zn(NO<sub>3</sub>)<sub>2</sub>. The binding stoichiometry between TPPS<sub>4</sub>-Zn(NO<sub>3</sub>)<sub>2</sub> and C<sub>14</sub>DMAO was calculated to be 1/2, suggesting that each TPPS<sub>4</sub>-Zn(NO<sub>3</sub>)<sub>2</sub> plane was connected with two C<sub>14</sub>DMAO molecules. X-ray diffraction (XRD) measurements were taken to reveal information on the molecular arrangement. In Fig. 3d and Fig. S6 (ESI†), the diffraction peak  $2\theta$  was  $2.64^\circ$ , suggesting that the unit-to-unit distance ( $\sim 33.44 \text{ \AA}$ ) might be the distance of each porphyrin planar.

Combined with the results of UV-vis, XPS, ITC, and XRD measurements, we speculate the structure model for the ternary-component helix of TPPS<sub>4</sub>-Zn(NO<sub>3</sub>)<sub>2</sub>-C<sub>14</sub>DMAO (Fig. S7, ESI†).

The coordination interaction plays a key role in the self-assembly, which correspondingly leads to a zinc ion coordinated with TPPS<sub>4</sub> and two C<sub>14</sub>DMAOs. There are still some uncoordinated C<sub>14</sub>DMAOs existing in the aggregates besides the C<sub>14</sub>DMAOs coordinated with the zinc porphyrin. Hydrophobic interaction is the driving force for self-assembly. The cooperative effect of coordination,  $\pi$ - $\pi$  and hydrophobic interactions is believed to trigger the ordered self-assembly of the ternary components helical structure. Furthermore, a similar helical structure can be acquired by replacing C<sub>14</sub>DMAO with C<sub>12</sub>DMAO (Fig. S8, ESI†).

In summary, a helical structure is successfully fabricated by the ternary components of TPPS<sub>4</sub>, Zn(NO<sub>3</sub>)<sub>2</sub> and C<sub>14</sub>DMAO in aqueous solution. The unit of TPPS<sub>4</sub>-Zn(NO<sub>3</sub>)<sub>2</sub>-C<sub>14</sub>DMAO is constructed through the coordination of a zinc ion to the porphyrin and a zinc ion to amphiphilic molecules. The delicately cooperative effect of coordination,  $\pi$ - $\pi$  and hydrophobic interactions accounted for the helical structure. Moreover, the helices retain the characteristic fluorescence of the porphyrin and exhibit a high conductive feature compared with other porphyrin tubes and ribbons previously reported. It is anticipated that the assembling helix with ternary components might have potential applications in photochemistry and electrical devices.

## Notes and references

- 1 K. Sugase, H. J. Dyson and P. E. Wright, *Nature*, 2007, **447**, 1021.
- 2 Y. Lin, A. Wang, Y. Qiao, C. Gao, M. Drechsler, J. Ye, Y. Yan and J. Huang, *Soft Matter*, 2010, **6**, 2031.
- 3 (a) S. M. Douglas, H. Dietz, T. Liedl, B. Hoegberg, F. Graf and W. M. Shih, *Nature*, 2009, **459**, 414; (b) R. V. Ulijn and A. M. Smith, *Chem. Soc. Rev.*, 2008, **37**, 664.
- 4 (a) M. A. Mateos-Timoneda, M. Crego-Calama and D. N. Reinhoudt, *Chem. Soc. Rev.*, 2004, **33**, 363; (b) L. C. Palmer and S. I. Stupp, *Acc. Chem. Res.*, 2008, **41**, 1674.
- 5 (a) E. G. Bellomo, M. D. Wyrsta, L. Pakstis, D. J. Pochan and T. J. Deming, *Nat. Mater.*, 2004, **3**, 244; (b) M. A. J. Gillissen, M. M. E. Koenigs, J. J. H. Spiering, J. Vekemans, A. R. A. Palmans, I. K. Voets and E. W. Meijer, *J. Am. Chem. Soc.*, 2014, **136**, 336.
- 6 A. L. Boyle, E. H. C. Bromley, G. J. Bartlett, R. B. Sessions, T. H. Sharp, C. L. Williams, P. M. G. Curmi, N. R. Forde, H. Linke and D. N. Woolfson, *J. Am. Chem. Soc.*, 2012, **134**, 15457.
- 7 L. Chen, K. S. Mali, S. R. Puniredd, M. Baumgarten, K. Parvez, W. Pisula, S. De Feyter and K. Muellen, *J. Am. Chem. Soc.*, 2013, **135**, 13531.
- 8 N. Giuseppone, J.-L. Schmitt and J.-M. Lehn, *J. Am. Chem. Soc.*, 2006, **128**, 16748.
- 9 H. Ozawa, H. Tanaka, M. Kawao, S. Uno and K. Nakazato, *Chem. Commun.*, 2009, 7411.
- 10 T. Sugimoto, T. Suzuki, S. Shinkai and K. Sada, *J. Am. Chem. Soc.*, 2007, **129**, 270.
- 11 K.-H. Chan, X. Guan, V. K.-Y. Lo and C.-M. Che, *Angew. Chem., Int. Ed.*, 2014, **53**, 2982.
- 12 D. Dolmans, D. Fukumura and R. K. Jain, *Nat. Rev. Cancer*, 2003, **3**, 380.
- 13 (a) M. J. Huang, L. Y. Hsu, M. D. Fu, S. T. Chuang, F. W. Tien and C. H. Chen, *J. Am. Chem. Soc.*, 2014, **136**, 1832; (b) T. Hasobe, A. S. D. Sandanayaka, T. Wada and Y. Araki, *Chem. Commun.*, 2008, 3372.
- 14 (a) S. J. Choi, Y. C. Lee, M. L. Seol, J. H. Ahn, S. Kim, D. I. Moon, J. W. Han, S. Mann, J. W. Yang and Y. K. Choi, *Adv. Mater.*, 2011, **23**, 3979; (b) H.-X. Ji, J.-S. Hu and L.-J. Wan, *Chem. Commun.*, 2008, 2653.
- 15 L. Feng, Z. Slanina, S. Sato, K. Yoza, T. Tsuchiya, N. Mizorogi, T. Akasaka, S. Nagase, N. Martin and D. M. Guldi, *Angew. Chem., Int. Ed.*, 2011, **50**, 5909.
- 16 A. D. Schwab, D. E. Smith, B. Bond-Watts, D. E. Johnston, J. Hone, A. T. Johnson, J. C. de Paula and W. F. Smith, *Nano Lett.*, 2004, **4**, 1261.
- 17 V. V. Roznyatovskiy, R. Carmieli, S. M. Dyar, K. E. Brown and M. R. Wasielewski, *Angew. Chem., Int. Ed.*, 2014, **53**, 3457.
- 18 S. R. Ahrenholtz, C. C. Epley and A. J. Morris, *J. Am. Chem. Soc.*, 2014, **136**, 2464.
- 19 (a) M. Khalid, J. S. Acuña, M. A. Tumelero, J. A. Fischer, V. C. Zoldan and A. A. Pasa, *J. Mater. Chem.*, 2012, **22**, 11340; (b) D. Yoon, S. B. Lee, K.-H. Yoo, J. Kim, J. K. Lim, N. Aratani, A. Tsuda, A. Osuka and D. Kim, *J. Am. Chem. Soc.*, 2003, **125**, 11062.
- 20 J. Rochford, D. Chu, A. Hagfeldt and E. Galoppini, *J. Am. Chem. Soc.*, 2007, **129**, 4655.
- 21 M. Fathalla, S. C. Li, U. Diebold, A. Alb and J. Jayawickramarajah, *Chem. Commun.*, 2009, 4209.
- 22 A. Rienzo, L. C. Mayor, G. Magnano, C. J. Satterley, E. Ataman, J. Schnadt, K. Schulte and J. N. O'Shea, *J. Chem. Phys.*, 2010, **132**, 084703.